First-Principles Calculations on the Emission Properties of Pristine and N-Doped Carbon Nanotubes

ARTICLE *in* THE JOURNAL OF PHYSICAL CHEMISTRY C · JANUARY 2009

Impact Factor: 4.77 · DOI: 10.1021/jp809277w

Article

First-Principles Calculations on the Emission Properties of Pristine and N-Doped Carbon Nanotubes

Chun Wang, Liang Qiao, Chaoqun Qu, Weitao Zheng, and Qing Jiang

J. Phys. Chem. C, **2009**, 113 (3), 812-818 • Publication Date (Web): 30 December 2008

ARTICLES

First-Principles Calculations on the Emission Properties of Pristine and N-Doped Carbon Nanotubes

Chun Wang,[†] Liang Qiao,[†,‡] Chaoqun Qu,[†] Weitao Zheng,*[,†] and Qing Jiang[†]

Department of Materials Science and Key Laboratory of Automobile Materials, MOE, Jilin University, Changchun 130012, People's Republic of China, and College of Science, Changchun University, Changchun 130022, People's Republic of China

Received: December 20, 2007; Revised Manuscript Received: December 1, 2008

The electronic structures and field-emission properties for pristine and N-doped capped single-walled carbon nanotubes (CNTs) are investigated on the basis of density functional theory. The emission currents from three types of orbitals in CNTs are calculated under the applied electric field. Upon N-doping, total current increases about 4 times under a lower electric field, and 1.5 times under a higher electric field. Comparison between the emission currents from different orbitals shows that the orbital induced by N-doping plays an important role in the emission property of N-doped CNT. The effect of the doping position on the emission property for N-doped CNT is discussed, and the optimal N-doping configuration is obtained.

1. Introduction

Since 1991,[1] carbon nanotubes (CNTs) have drawn particular attention due to their unique geometrical structures and novel physical properties.[2,3] As a kind of quasi-one-dimensional material, CNTs are considered as field electron emitters,[4] nanoheterojunctions,[5] scanning tunneling microscopy tips,[6] and structural reinforcement fibers.[7] Among the proposed applications, field-emission displays with CNT cold cathodes are the most promising and considered as the next-generation flat-panel displays.[8] As compared to conventional metallic field-emission tips, CNTs as field-emission electron source have many advantages: unusually high aspect ratio, high chemical stability, low extracting field, high current density, as well as long operating time.

The application of CNTs as field emitters[3] is based on the electrical properties of CNTs, which strongly depend on the microscopic electronic structures of CNTs. Thus, the control of the electronic structures of CNTs is of great technological importance. Doping CNTs with other elements is the best way to accomplish this goal, wherein nitrogen atom is the most common candidate of n-type dopant for carbon materials, which can modify the electronic structures of CNTs by introducing donor states near the Fermi level. N-doped CNTs have been synthesized by several groups,[9−12] and the existing experimental investigations indicate that N-doped CNTs show enhanced electron field emission and special emission properties.[13−16] It is found that N-doped CNTs exhibit higher current density and stable electron field emission at lower turn-on voltage when compared to pristine CNTs.[17] However, the mechanism for these enhanced emissions is yet to be understood.

First-principles calculations have been successfully used to identify the electronic structures and electronic properties of CNTs, and the electronic structures at CNTs tips and field-emission behaviors of CNTs have been reported.[18,19] On the other hand, as compared to pristine CNTs, the field-emission properties of N-doped CNTs are also investigated theoretically.[20,21] In our recent paper,[22] the structures and the electronic properties of N-doped CNTs under an applied electric field have been explored by the first-principles density-functional theoretical (DFT) simulation. The results show that the gaps of N-doped CNTs are reduced significantly when compared to pristine CNT, and the donor states induced by the N atoms can be observed near the Fermi level. Although our and other theoretical investigations have demonstrated the enhanced field-emission properties of N-doped CNTs, the mechanism of this enhancement is not clearly revealed. Furthermore, because the actual emission current depends strongly on the local electric field and the distribution of the electrons near the emission side, which could be affected by the doping configuration, the evaluation for the emission current is thus required for a complete understanding of the emission behavior.[21]

The aim of this work is to study the field-emission properties for N-doped (5, 5) CNTs by calculating their emission currents under the applied electric field. The different doping positions of nitrogen atom are chosen and the currents are calculated under different electric field strengths, to study the effect of both the N atom and the strength of the applied electric field on the field-emission properties for N-doped CNTs.

2. Theoretical Methods

In this work, a finite-length capped (5, 5) single-walled CNT with nitrogen substitutional atom was considered. The diameter of armchair (5, 5) CNT was 6.8 Å, which was similar to that of C60. The capped CNT was represented by eight layers of carbon rings along the tube axis with one end capped by half of C60

* Corresponding author. Tel.: +86-431-85168246. Fax: +86-431-85168246. E-mail: wtzheng@jlu.edu.cn.
† Jilin University.
‡ Changchun University.

10.1021/jp809277w CCC: $40.75
Published on Web 12/30/2008

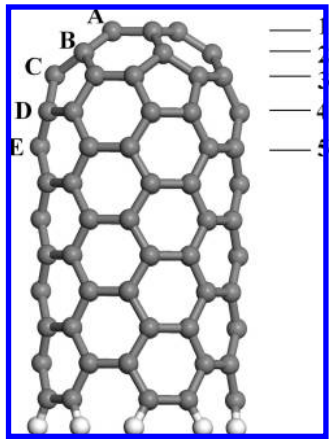

Figure 1. Geometrical structure of the CNT used in our calculation. The letters denote the different doping positions of the substitutional nitrogen atom in each atomic layer, which is indexed by the number.

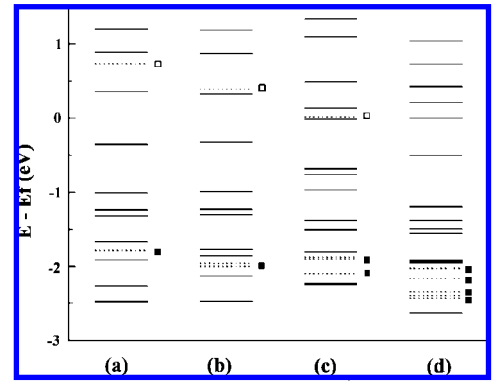

Figure 2. Energy levels for pristine CNT without an applied electric field (a) and at an electric field of 0.3 V/Å (b) and 1 V/Å (c). The energy levels for the first-layer-doped CNT are shown in (d). The "■" denote the energy levels for the occupied orbitals localized at the tip, while the "□" denote the evolution of LUMO+1 orbital under the electric field. The corresponding energy levels are drawn by dotted lines for clarity. Fermi level is fixed at the zero of energy axes.

and hydrogen atoms saturating the dangling bonds at the other end of the CNTs, to increase the chemical stability of the structures and emulate infinite CNTs. The nanotube in this model was longer than that in our previous study[22,23] for minimizing the finite-size effect. The doped CNT was the capped CNT with direct substitution of one carbon atom by one nitrogen atom in the hexagonal lattice, which can lead to different doping positions of the doped CNTs. Pristine CNT was also considered to compare to the doped ones. The final system contained 120 atoms with the two carbon layers at the bottom fixed during the whole simulation to mimic the presence of a long CNT below the tip in experiments. The geometrical structure of (5, 5) CNT used in the calculation was shown in Figure 1. The numbers denote the different atomic layers of CNT, and the letters denote the different doping positions of the substitutional nitrogen atom in each atomic layer. Five different configurations for N-doped CNTs were considered in the present work.

To obtain the exact and detailed information about the geometrical structures and electronic structures of N-doped CNTs, the doped CNTs were first optimized to get the most stable geometrical structure before the electronic property calculation was performed. All of the calculations were carried out using first-principles DFT provided by DMOL^3 code.[24,25] In our DFT calculations, the all-electron Kohn−Sham wave functions were expanded in the local atomic orbital basis set. In the double numerical basis set, the 2s and 2p carbon orbitals were represented by two wave functions each, and a 3d-type wave function on each carbon atom was used to describe the polarization. The generalized gradient approximation (GGA) with the Perdew−Burke−Ernzerhof[26] correlation gradient correction was used to describe the exchange and correlation energy in all calculations. The optimization of the structure was done until the change in energy was less than 10^{-5} hartree.

To study the field-emission properties of CNTs, a uniform electric field was applied along the CNT axis, and then the electronic properties were computed after the structural relaxation under the electric field. The structural changes were rather small under the applied electric field. The emission currents of CNTs under the applied fields were calculated using the method presented by Khazaei et al.,[27] which was based on first-principles calculations. These calculations had been successfully performed to study the emission current from both pristine[28] and Cs-doped CNTs.[29] In this method, the necessary data for calculating emission currents were potential energy barrier, orbital energy, and orbital electronic density. All of these above were obtained from DFT calculations. The emission current from a single orbital was proportional to the probability of electron tunneling from this orbital to vacuum, electronic density at the emission points, and the occupation for this orbital. The supercell is discretized by introducing a fine grid, and currents along individual grid lines parallel to the emission direction were calculated according to the DFT results. The total current was then obtained by summing the currents along these grid lines. The details of this calculation can be found in ref 27.

3. Results and Discussion

3.1. Electronic Structures of Pristine and N-Doped CNTs.

First, the electronic structure of pristine CNT is investigated. The calculated energy levels for CNT under the electric fields with different strengths are shown in Figure 2. It is found that both the highest occupied molecular orbital (HOMO) and the lowest unoccupied molecular orbital (LUMO) for pristine CNT are extended states in the sidewall without an electric field. Furthermore, we find that HOMO still locates at the sidewall of CNT, but LUMO is localized on the tip of CNT under an electric field of 1 V/Å. The change in the distribution of LUMO has been related to the charge transfer between occupied and unoccupied orbitals,[30,31] but the exact reason is seldom discussed. We suggest that LUMO localized on the tip of CNT under the electric field may evolve from the higher energy level for CNT without an electric field. According to our calculation, the lowest unoccupied orbital localized at the tip of isolated CNT is the first orbital above LUMO (LUMO+1). When the electric field is applied, the potential energy for the electron at the tip decreases as compared to that in the sidewall. Thus, the energy for LUMO+1 orbital on the tip decreases as compared to that for HOMO and LUMO in the sidewall, which is supported by the energy levels under an electric field of 0.3 V/Å in Figure 2. When the electric field strength is large enough, the energy of this orbital becomes lower than the unoccupied orbital in the sidewall, and this orbital becomes LUMO. Simultaneously, it can be explained that the gap of CNT reduces under an electric field of 1 V/Å. As shown in Figure 2, the occupied orbitals localized on the tip locate at about 1.5 eV below HOMO.

We have calculated the electronic structures for N-doped CNTs, and the energy levels for the first-layer-doped CNT are shown in Figure 2. From the energy levels near the Fermi level,

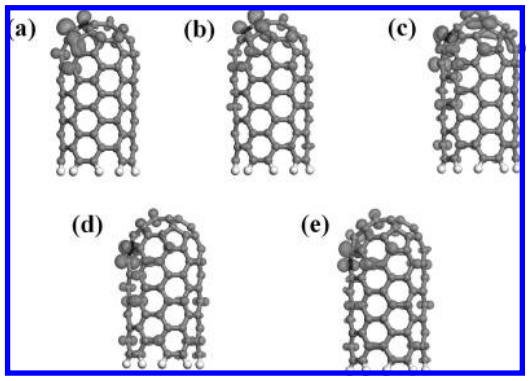

Figure 3. Side view of coupled orbitals in N-doped CNTs with different configurations. From (a) to (e), the doping positions are consistent with those indexed in Figure 1.

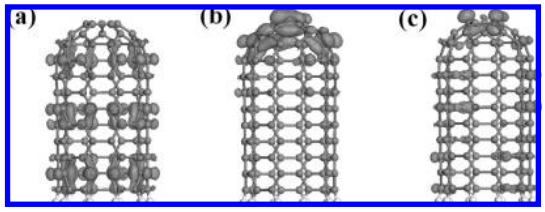

Figure 4. Side view of three typical orbitals in pristine CNT: HOMO (left, T1 orbital), LUMO+1 (center, T2 orbital), and the highest occupied orbitals localized at the tip (right, T3 orbital).

we find that N atoms induce orbitals located above HOMO for pristine CNT, which results in an increase in the Fermi level. Noticeably, these orbitals are not only localized at the cap of the tube, but also have a distribution at the sidewall (Figure 3), especially for the configurations where the N atoms locate near the sidewall of CNTs. These kinds of states are called "coupled states",[22] having mixed properties with both the localized states and the extended states, and have been expected to play important roles in the emission properties of N-doped CNTs. Interestingly, the degeneracy of the occupied orbitals localized on the tip becomes fully released after the N-doping, as shown in Figure 2. This is because the C_{5v} symmetry of the CNT has been destroyed after doping, and then the degeneracy is released.

3.2. Emission Properties of CNTs under a Low Electric Field. To study the emission properties of CNT, three types of orbitals are investigated emphatically. First, the extended orbitals locate near the Fermi level and distribute in the sidewall (T1 orbitals). Second, the localized orbitals locate near the Fermi level and distribute at the tip (T2 orbitals). Finally, the localized orbitals locate below the Fermi level and distribute at the tip (T3 orbitals). The shapes of typical orbitals for these types are shown in Figure 4. The coupled orbitals induced by N-doping mainly locate around the N atoms in the tip (Figure 3) and should be considered as T2 orbitals.

The emission currents from these three types of orbitals for pristine and N-doped CNT are calculated by the method presented by Khazaei.[27] Total currents under a lower electric field (0.3 V/Å) are shown in Figure 5a. We find that the current increases drastically after N-doping; the field-emission properties of carbon nanotubes can be enhanced by N-doping, which is consistent with our previous investigation.[22] The currents from different types of orbitals are shown in Figure 5b. For pristine CNTs, the result reveals that the emission current mainly comes from the T1 orbitals, while the contributions from the other two types are quite small. The energies for T3 orbitals are much lower than those of T1 orbitals, which results in much longer tunneling distances and lower tunneling probabilities for this

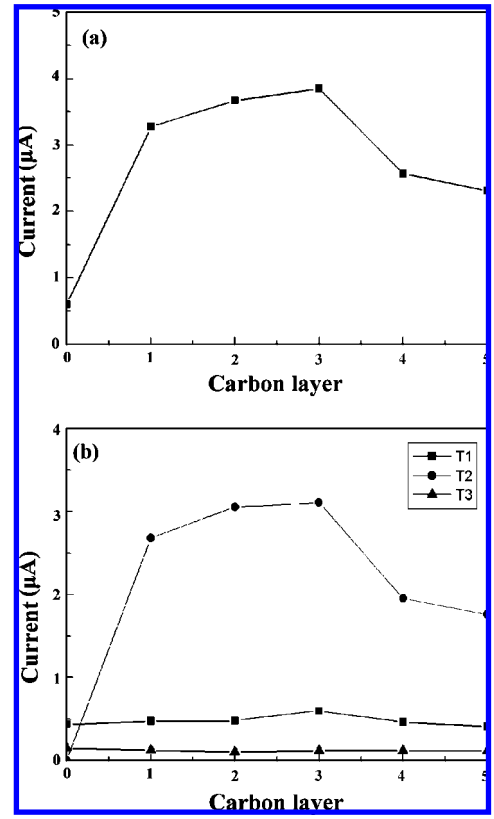

Figure 5. Calculated total currents for N-doped CNTs under a lower electric field (a). The abscissa denotes the doping layer of CNT, and the layer "zero" denotes pristine CNT. Currents from different types of orbitals are shown in (b).

type of orbital under a lower electric field. Consequently, the emission currents from T3 orbitals are restricted by the tunneling probability. On the other hand, T2 orbitals are unoccupied orbitals for pristine CNT. The energy differences between these orbitals and the Fermi level are quite large under a lower electric field, which results in small occupations for these orbitals according to the Fermi−Dirac distribution. Therefore, the currents from T2 orbitals are negligible. After N-doping, the currents from T1 and T3 orbitals change slightly [Figure 5b], and the increase in total current is mainly contributed by the coupled orbitals (belongs to T2). Hence, we focus on the emission properties of this type of orbital.

The calculated energy levels of coupled orbitals for N-doped CNTs with different configurations under an electric field of 0.3 V/Å are shown in Figure 6, which reveals that the energies for coupled orbitals are all higher than HOMO of pristine CNT. In addition, it is found that the coupled orbital for CNT with N-doping near the emission side (substituted at the first or second layer) has a lower energy, while that for CNT with N atom doping near the sidewall (substituted at the third, forth, or fifth layer) has a higher energy. Noticeably, such a trend appears only when the electric field is applied (Figure 6) and can be ascribed to the applied electric field. As mentioned above, the orbital induced by N-doping locates around the N atom (Figure 3). As a result, when the N-doping position shifts toward the emission side, the coupled orbital shifts toward the tip correspondingly. Under the applied electric field, the potential energy for the electron near the emission side is lower than that in the sidewall. Consequently, the N atom doped near the tip induces a lower energy level than does that near the sidewall.

The calculated tunneling probability patterns for coupled orbitals under an electric field of 0.3 V/Å are shown in Figure

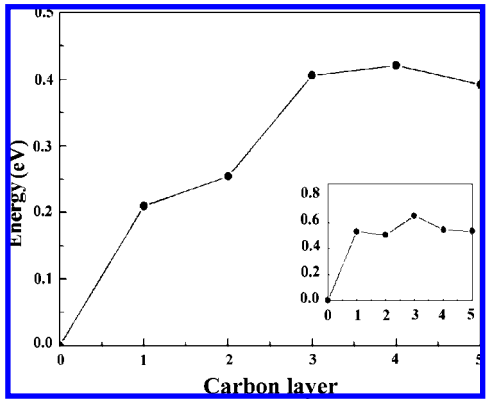

Figure 6. Energy levels for coupled orbitals of N-doped CNTs with various doping configurations under an electric field of 0.3 V/Å. The abscissa denotes the doping layer of CNT, and the layer "zero" denotes pristine CNT. The energy is relative to the energy level of HOMO for pristine CNT. The inset shows the energy levels without an applied electric field.

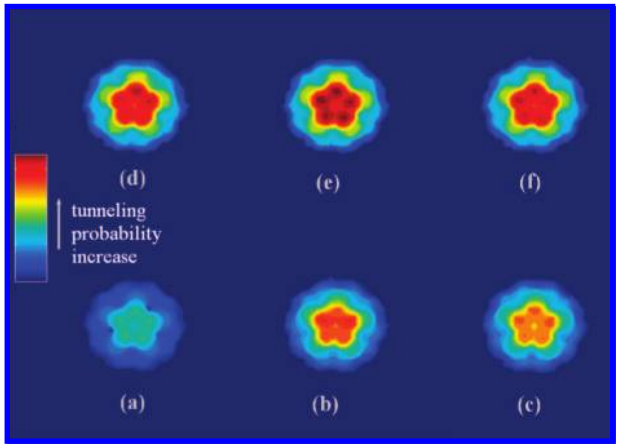

Figure 7. Tunneling probability patterns for (a) HOMO of pristine CNT, and (b)−(f) coupled orbitals of first- to fifth-layer-doped CNTs under an electric field of 0.3 V/Å. Arrow in the color map denotes an increase of the tunneling probability.

7. The tunneling probability pattern for HOMO of pristine CNT is also given for comparison. The emission sites with the highest tunneling probabilities locate at the pentagon on the tip of the CNT, which results from the sharp configuration and the shortest tunneling distance for these positions. The tunneling probability for pristine CNT is much smaller than that of N-doped CNT with any configurations, which can be attributed to the increase in the energy of coupled orbital induced by N-doping. Furthermore, the coupled orbital is localized with a higher electronic density at the tip and larger emission area as compared to T1 orbitals. These features lead to that the current from the coupled orbital is much larger than that from the other orbitals and plays a dominant role in total current under a lower electric field.

In Figure 7, we also find that the coupled orbital for CNT with N-doping near the emission side shows a lower tunneling probability, while that for CNT with N atom doping near the sidewall has a higher tunneling probability. This trend can be explained by the energy levels for these orbitals (Figure 6). Our calculation suggests that the doping configuration can influence not only the electron distribution but also the tunneling probability for the coupled orbital.

3.3. Emission Properties of CNTs under a High Electric Field. To study the effect of the applied electric field on the emission properties for N-doped CNTs, a higher electric field of 1 V/Å is applied, and the calculated total currents from three

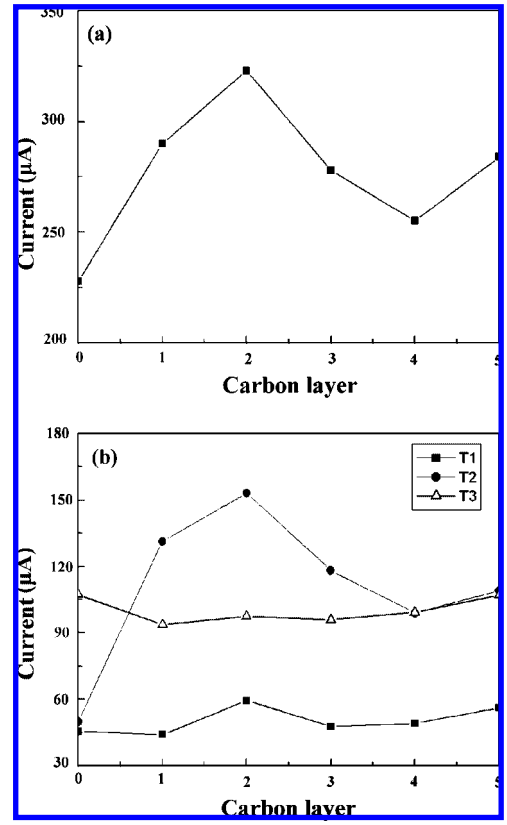

Figure 8. Calculated total currents for N-doped CNTs under a higher electric field (a). The abscissa denotes the doping layer of CNT, and the layer "zero" denotes pristine CNT. Currents from different types of orbitals are shown in (b).

types of orbitals are shown in Figure 8a. Calculations on the currents show that the currents increase after N-doping. However, we find that the emission current only increases no more than 1.5 times under a higher electric field after doping, while it increases about 4 times under a lower electric field (Figure 5a). The increase in total current is also mainly contributed by the coupled orbitals (T2) under a higher electric field (Figure 8b). However, the emission current from T3 orbitals has a large contribution to total current for CNTs under a higher electric field, which is less affected by N-doping. Therefore, the increase in total current from T2 orbitals is less pronounced than that under a lower electric field.

T3 orbitals locate deeply below Fermi level, and the tunneling probabilities are quite small for this type of orbital under a lower electric field. However, under a strong applied electric field, the structure-vacuum barrier height decreases at very short distances near the nanotube surface.[32,33] Consequently, the tunneling probability of the electronic states located deeply below HOMO increases, resulting in a large contribution of deep electronic states in total current.[28] Furthermore, T3 orbitals show larger electronic densities at the emission side and are substantially exposed to the electric field, which results in larger emission areas. Therefore, the currents from this type of orbitals become larger than that of T1 orbitals.

Another difference between the emission currents under a higher and lower electric field comes from T2 orbitals of pristine CNT, which locate above the Fermi level. The occupations for T2 orbitals are negligible under a lower electric field, which results in a negligible current from these orbitals. However, as discussed above, when the strength of the applied electric field increases, the energy levels for the unoccupied orbitals located

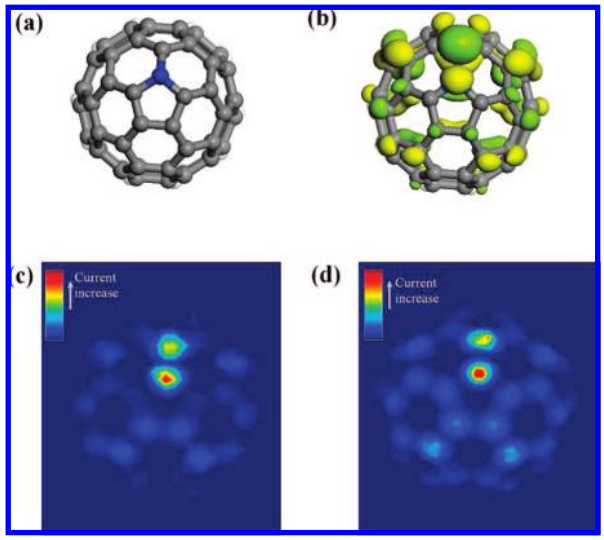

Figure 9. From (a) to (d): top view of the structure for CNT with N-doped in the first layer (a), top view of the electron distribution for coupled orbital (b), and total current patterns under an electric field of 0.3 V/Å (c) and 1 V/Å (d). Arrows in the color maps denote an increase of the current.

in the cap (T2 orbitals) shift toward the Fermi level. This results in an increase in the occupation for these orbitals, and hence the current from T2 orbitals increases significantly under a higher electric field.

It is observed that the largest current comes from the second-layer-doped CNT under a higher electric field (Figure 8). Under a lower electric field, however, the largest current comes from the third-layer-doped CNT with N atom, as shown in Figure 5a. Comparing the coupled orbitals for the second- and third-layer-doped CNTs, the former has a relative larger charge distribution on the tip (Figure 3), while the latter orbital shows a higher tunneling probability (Figure 7). Under a lower electric field, wherein the tunneling probability is the bottleneck for field emission, the emission current from the orbital of third-layer-doped CNT is larger. In contrast, the differences between the tunneling probabilities for the orbitals with similar energies are fully reduced under a higher field. Therefore, the current from the orbital of second-layer-doped CNT becomes larger, which shows a larger electronic density at the tip. The electronic origin of the difference in the field-emission properties of N-doped CNT is related to the nonbonding pair state and the antibonding state induced by N atom, which are responsible for the reduction of work function under proper electric field.[34,35]

The total current patterns for the first-layer-doped CNT under a lower and higher electric field are shown in Figure 9. The top view for the coupled orbital and the structure of this tube is also given. Under a low electric field, the emission does not distribute over the whole cap. This is because most of the emission current comes from HOMO (the coupled orbital) and very few energy levels below HOMO under a lower electric field. Thus, the emission pattern resembles the shape of the coupled orbital. In contrast, many electronic states, including the occupied orbitals located in the cap (T3 orbitals), contribute to the total current under a higher electric field. This leads to that the electrons are emitted from different positions of the cap and the total current distributes over the whole cap. From the total current patterns for both a higher and a lower electric field, it is observed that the current patterns around the doping site are markedly larger than the other positions. This suggests that it is feasible to explore the doping configurations of nanotubes through the experimental field-emission patterns.

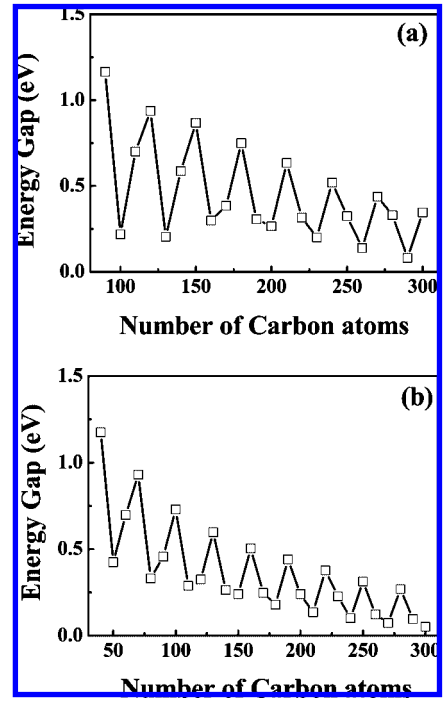

Figure 10. Energy gap versus the number of carbon atoms for (a) capped CNT and (b) open ended CNT, where the energy gap is calculated with DFT and TB approximation, respectively.

3.4. Length Effect. In this section, we investigate the finite-length effect on the field-emission properties for capped CNT, and we first examine the effect of the tube length on the electronic structure. As mentioned above, our capped CNT model is represented by eight layers of carbon rings along the tube axis with one end capped by half of C60, which consists of 110 carbon atoms. To explore the size-dependent features for capped CNTs, we gradually change the number of carbon ring layers from 6 to 27, wherein the number of carbon atoms changes from 90 to 300. The structure and electronic properties for these finite-length CNTs are calculated with the same theoretical method used in the previous section. Figure 10a shows the calculated energy gap as a function of the number of carbon atoms for capped CNT. Our calculations reveal that the energy gap for capped CNT exhibits a regular oscillation upon increasing the nanotube length. Furthermore, a tendency to reduce the gap is found when the tube length increases. To clarify whether this phenomenon originated from the tube sidewall or from the interactions between sidewall and cap, we have calculated the energy gaps of open ended CNTs with different lengths. This calculation is performed with semi-empirical tight-binding (TB) potential parametrized by Xu et al.[36] for simplification, and the calculated energy gap versus the number of carbon atoms is shown in Figure 10b. Although different theoretical methods are used, similar oscillations in the energy gap are found for open ended CNT and capped CNT. This result implies that this oscillation in energy gap for capped CNT originates from the quantum confinement effect in the sidewall.

We have also investigated the length-dependent features in the field-emission properties for capped CNT by calculating the emission currents from CNTs with different lengths. As we focus on the emission properties of N-doped CNT in the present work, the first-layer-doped CNT model is adopted, and the number of carbon layers increases gradually from 8 to 30 in this calculation. The N-doped CNTs with different lengths have been relaxed under the electric field of 1 V/Å before the

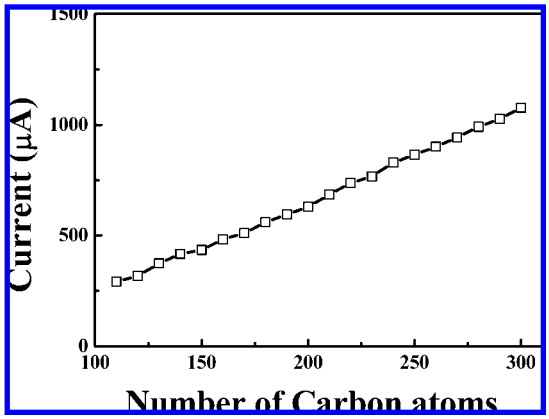

Figure 11. Calculated emission current versus the number of carbon atoms under the electric field of 1 V/Å for N-doped CNT.

electronic structure and field-emission property calculation. The calculation is performed with the DFT method, and the calculated emission current versus the number of carbon atoms is shown in Figure 11. An interesting finding is that, different from the length-dependent features in the electronic structure of CNT (Figure 10), there is no oscillation in the emission current when the nanotube length increases. This is because, in our present method, the emission current is mainly dependent on the localized states and the local electric potential around the cap region, which are less sensitive to the tube length. The states in the tube sidewall, which are affected by the quantum confinement effect and result in the oscillation in the energy gap, only play a minor role in the calculated emission current. In Figure 11, the emission current shows a steady increase with increasing tube length. We propose that this phenomenon is related to our theoretical model. In our present work, a uniform electric field, rather than a fixed bias voltage, is applied along the CNT axis. When the tube length increases, the electric potential difference between the cap and open ended region increases. Therefore, more electrons will transfer from the sidewall to the cap region, resulting in an increase in the calculated emission current.

Finally, we discuss the availability of the finite-length CNT model in understanding the field-emission properties for real CNTs. Although our calculations reveal that the electronic structure changes drastically with an increase in tube length (Figure 10a), we have found that this effect only originated form electronic states in sidewall, and the calculated field-emission current does not show this tendency, because this emission current is mainly governed by the local states around the cap region. Therefore, a finite-length CNT model can be used to investigate the emission properties for real CNTs, because this model can deal with the local electronic states and electric potential in the tip region of real CNTs.[37]

3.5. Effect of the Doped N Content. Because our present work focuses on the effect of doping position on the emission properties for N-doped CNT, the CNT model with only one substitutional nitrogen atom is adopted. However, we have previously calculated the electronic properties for infinite-length CNT with a relatively high N content.[38] It is found that when the nitrogen atoms are far apart, the calculated electronic structure is similar to that for the tube containing one nitrogen atom, except for an increase in the impurity peak in the electron density of states (DOS), induced by N-doping. In this case, the interaction between nitrogen atoms almost does not influence the emission property of N-doped CNT. On the other hand, due to the interaction between nitrogen atoms, the impurity peak shifts toward the valence band or conduction band, which depends on the different configurations in which N atoms occupy different sites, when the impurity N atoms are near each other. In this case, the effect of the doped N content on the emission properties of N-doped CNTs is complex, which will be explored in detail in our future work.

4. Conclusions

First-principles calculations can be used to study the field-emission properties for pristine and N-doped CNTs. Pristine CNT exhibits a semiconducting property with a finite value of energy gap, which can be attributed to the finite length for the theoretical model of capped CNT. LUMO for pristine CNT shifts from the sidewall to the tip under the applied electric field. This results from the shift of higher energy level rather than the charge transfer, which also leads to a decrease in energy gap under the electric field. Upon N-doping, the emission current for CNTs increases about 4 times under a lower electric field, and 1.5 times under a higher electric field. The coupled orbital induced by N-doping plays an important role in the emission properties of CNTs, especially under a lower electric field. Different doping configurations can influence both the electron distribution and the tunneling probability of coupled orbital, and hence affect the emission current. The optimal N-doping position is the second layer and third layer, respectively, under a higher and a lower electric field. The total current distributes over the whole cap only when a high electric field is applied, and the current around the doping site is markedly larger than in the other positions. These results reveal the role of nitrogen doping in enhancing the field-emission properties of CNTs and provide potential applications for N-doped CNTs.

Acknowledgment. We gratefully appreciate the financial support by the National Natural Science Foundation of China under Grant No. 50525204, the National Key Basic Research and Development Program (grant no. 2004CB619301), and the Teaching and Research Award Program for the Outstanding Young Teachers in High Education Institutions (no. 2002359).

References and Notes

(1) Iijima, S. *Nature* **1991**, *354*, 56.
(2) Dresselhaus, M. S.; Dresselhaus, G.; Saito, R. *Carbon* **1995**, *33*, 883.
(3) Sun, C. Q.; Bai, H. L.; Tay, B. K.; Li, S.; Jiang, E. Y. *J. Phys. Chem. B* **2003**, *107*, 7544.
(4) Rinzler, A. G.; Hafner, J. H.; Nikolaev, P.; Lou, L.; Kim, S. G.; Tománek, D.; Nordlander, P.; Colbert, D. T.; Smalley, R. E. *Science* **1995**, *269*, 1550.
(5) Hu, J. T.; Ouyang, M.; Yang, P. D.; Lieber, C. M. *Nature* **1999**, *399*, 48.
(6) Dai, H. J.; Hafner, J. H.; Rinzler, A. G.; Colbert, D. T.; Smalley, R. E. *Nature* **1996**, *384*, 147.
(7) Treacy, M. M. J.; Ebbesen, T. W.; Gibson, J. M. *Nature* **1996**, *381*, 678.
(8) Wang, Q. H.; Setlur, A. A.; Lauerhaas, J. M.; Dai, J. Y.; Seelig, E. W.; Chang, R. P. H. *Appl. Phys. Lett.* **1998**, *72*, 2912.
(9) Golberg, D.; Bando, Y.; Bourgeois, L.; Kurashima, K.; Sato, T. *Carbon* **2000**, *38*, 2017.
(10) Czerw, R.; Terrones, M.; Charlier, J. C.; Blasé, X.; Foley, B.; Kamalakaran, R.; Grobert, N.; Terrones, H.; Tekleab, D.; Ajayan, P. M.; Blau, W.; Rühle, M.; Carroll, D. L. *Nano Lett.* **2001**, *1*, 457.
(11) Kim, S. Y.; Lee, J. Y.; Na, C. W.; Park, J.; Seo, K.; Kim, B. *Chem. Phys. Lett.* **2005**, *413*, 300.
(12) Liu, J.; Webster, S.; Carroll, D. L. *Appl. Phys. Lett.* **2006**, *88*, 213119.
(13) Chan, L. H.; Hong, K. H.; Xiao, D. Q.; Hsieh, W. J.; Lai, S. H.; Shih, H. C.; Lin, T. C.; Shieu, F. S.; Chen, K. J.; Cheng, H. C. *Appl. Phys. Lett.* **2003**, *82*, 4334.

(14) Srivastava, S. K.; Vankar, V. D.; Rao, V. D. S.; Kumar, V. *Thin Solid Films* **2006**, *515*, 1851.
(15) Doytcheva, M.; Kaiser, M.; Verheijen, M. A.; Reyes, M. R.; Terrones, M.; de Jonge, N. *Chem. Phys. Lett.* **2004**, *396*, 126.
(16) Sharma, R. B.; Late, D. J.; Joag, D. S.; Govindaraj, A.; Rao, C. N. R. *Chem. Phys. Lett.* **2006**, *428*, 102.
(17) Wang, X.; Liu, Y.; Zhu, D.; Zhang, L.; Ma, H.; Yao, N.; Zhang, B. *J. Phys. Chem. B* **2002**, *106*, 2186.
(18) Carroll, D. L.; Redlich, P.; Ajayan, P. M.; Charlier, J. C.; Blasé, X.; De Vita, A.; Car, R. *Phys. Rev. Lett.* **1997**, *78*, 2811.
(19) Tamura, R.; Tsukada, M. *Phys. Rev. B* **1995**, *52*, 6015.
(20) Zhang, G.; Duan, W.; Gu, B. *Appl. Phys. Lett.* **2002**, *80*, 2589.
(21) Ahn, H. S.; Lee, K. R.; Kim, D. Y.; Han, S. *Appl. Phys. Lett.* **2006**, *88*, 093122.
(22) Qiao, L.; Zheng, W. T.; Xu, H.; Zhang, L.; Jiang, Q. *J. Chem. Phys.* **2007**, *126*, 164702.
(23) Qiao, L.; Zheng, W. T.; Wen, Q. B.; Jiang, Q. *Nanotechnology* **2007**, *18*, 155707.
(24) Delley, B. *J. Chem. Phys.* **1990**, *92*, 508.
(25) Delley, B. *J. Chem. Phys.* **2000**, *113*, 7756.
(26) Perdew, J. P.; Burke, K.; Ernzerhof, M. *Phys. Rev. Lett.* **1996**, *77*, 3865.
(27) Khazaei, M.; Farajian, A. A.; Kawazoe, Y. *Phys. Rev. Lett.* **2005**, *95*, 177602.
(28) Khazaei, M.; Dean, K. A.; Farajian, A. A.; Kawazoe, Y. *J. Phys. Chem. C* **2007**, *111*, 6690.
(29) Khazaei, M.; Kawazoe, Y. *Surf. Sci.* **2007**, *601*, 1501.
(30) Kim, C.; Kim, B.; Lee, S. M.; Jo, C.; Lee, Y. H. *Appl. Phys. Lett.* **2001**, *79*, 1187.
(31) Kim, C.; Kim, B.; Lee, S. M.; Jo, C.; Lee, Y. H. *Phys. Rev. B* **2002**, *65*, 165418.
(32) Binh, V. T.; Purcell, S. T.; Garcia, N.; Doglioni, J. *Phys. Rev. Lett.* **1992**, *69*, 2527.
(33) Fransen, M. J.; van Rooy, T. L.; Kruit, P. *Appl. Surf. Sci.* **1999**, *146*, 312.
(34) Sun, C. Q. *Appl. Phys. Lett.* **1998**, *72*, 1076.
(35) Zheng, W. T.; Sun, C. Q. *Prog. Solid State Chem.* **2006**, *34*, 1.
(36) Xu, C. H.; Wang, C. Z.; Chan, C. T.; Ho, K. M. *J. Phys.: Condens. Matter* **1992**, *4*, 6047.
(37) Maiti, A.; Andzelm, J.; Tanpipat, N.; Allmen, P. *Phys. Rev. Lett.* **2001**, *87*, 155502.
(38) Yu, S. S.; Wen, Q. B.; Zheng, W. T.; Jiang, Q. *Nanotechnology* **2007**, *18*, 165702.

JP809277W